2007 IEEE International Conference on
Robotics and Automation
Roma, Italy, 10-14 April 2007

Obstacle Detection of a Humanoid on a Plane Using a Relative Disparity Map Obtained by a Small Range Image Sensor

Naotaka Hikosaka, Kei Watanabe and Kazunori Umeda

Abstract— **In this paper, methods for detecting obstacles on a plane using a relative disparity map (RDMap) are proposed and discussed. The RDMap, which was formerly introduced by the author Umeda, is relative to a plane that is observed at first as the reference. It has an interesting feature that a plane in real 3D space also becomes a plane in the map, and has homogeneous characteristics compared to an ordinary range image. The proposed methods work even when the pose of the sensor changes significantly, which is the case in humanoid walking. First, a method to detect planar regions and obstacles by fitting a plane to the RDMap and a method to obtain the pose parameters from the RDMap are introduced. Fundamental experiments are then conducted to verify that a plane in real 3D space becomes a plane in the RDMap and that obstacles can be detected using the residual sum of squares for the fitted plane, and measurement errors in pose parameters are then evaluated. Finally, an experimental system with a humanoid and a small range image sensor is constructed, and it is demonstrated that the humanoid can detect obstacles on a plane by the proposed methods while walking.**

I. Introduction

Robots are currently being used in human environments, such as offices and houses Because there are many obstacles in these environments, a robot must be able to detect planar regions in which it can move [1], [2]. For this purpose, three-dimensional (3D) information is necessary, and range images, which are the most typical, are effective as the 3D information. Many methods to acquire range images have been studied. For robot applications, real-time sensing is necessary, and some methods can realize real-time range imaging. Stereo vision is very common and commercial sensors are available [3]. However, stereo vision has an essential problem, i.e., stereo correspondence problem [4]. In [5], a 3D map is reconstructed using stereo vision. Although a humanoid can walk through a room full of objects to reach its goal in the experiment, the problem of stereo correspondence is avoided by putting artificial patterns on most of the obstacles.

On the other hand, active sensors can obtain 3D information of an environment more robustly without the correspondence problem. Beraldin et al. realized video-rate range imaging by scanning a laser spot using their synchronized laser scan technique [6]. Kanade [7] developed a special imaging detector and realized real-time imaging by scanning a laser slit with the detector. Nakazawa [8] constructed a sensor without scanning by projecting multi-spots. The spot pattern was generated using a fiber grating and a laser. This type of sensor has been used for some robotic applications, such as object recognition [9] and navigation of a mobile robot [10].

In this study, we also use a range image sensor using a multi-spot laser projector [11], [12]. This sensor is suitable for mobile robots, including humanoids, because it is small. Even a small robot can carry it, and real-time range imaging is possible. In most studies in which range images are applied, actual range information is used. However, obtaining actual range images requires strict calibration. In addition, the density of points of an actual range image is not homogenous, i.e., when the distance is larger, the density becomes lower and the measured distance has larger error. We proposed a relative disparity map (RDMap) that overcomes these problems [11] and showed that a wheeled mobile robot can avoid obstacles using the map.

In this paper, we propose methods of recognizing obstacles on a plane using an RDMap, even when the pose of a sensor changes significantly, which occurs in humanoid walking. The obstacles we deal with are anything that is off the plane in the sensor's field of view. Firstly, the use of an RDMap is discussed. Fundamental experiments are conducted to demonstrate the effectiveness of the method for detecting a plane and obstacles. Finally, experiments with a humanoid are conducted to demonstrate obstacle recognition while walking with the proposed method .

II. Relative disparity map

A. What is a relative disparity map? [11]

An RDMap is defined as follows. A range image sensor observes a plane as a reference in advance, and, when it observes a target scene, it detects disparities that are relative to the reference plane. When the range image sensor with multi-spots is used, the RDMap is easily measured as the shifts of the projected spots. This is illustrated in Fig.1.

The pose of a sensor for a plane (typically a floor) can be given as shown in Fig.2. The height from the plane is h; the angle between the z-axis (optical axis) of the sensor and the plane is θ; and the rotation angle of the sensor around its z-axis is ϕ. Supposing the measuring direction (of each spot) is $\begin{bmatrix} s & t & 1 \end{bmatrix}^T$ as shown in Fig.3, the pose parameters of the reference plane are h_0, θ_0, ϕ_0, and the disparity of the reference plane for infinite distance is $k_0(s,t)$. Then, the

N. Hikosaka and K. Watanabe are with the Course of Precision Engineering, School of Science and Engineering, Chuo University, 1-13-27 Kasuga, Bunkyo-ku, Tokyo 112-8551, Japan hikosaka@sensor.mech.chuo-u.ac.jp

K. Umeda is with the Department of Precision Mechanics, Faculty of Science and Engineering, Chuo University, 1-13-27 Kasuga, Bunkyo-ku, Tokyo 112-8551, Japan umeda@mech.chuo-u.ac.jp

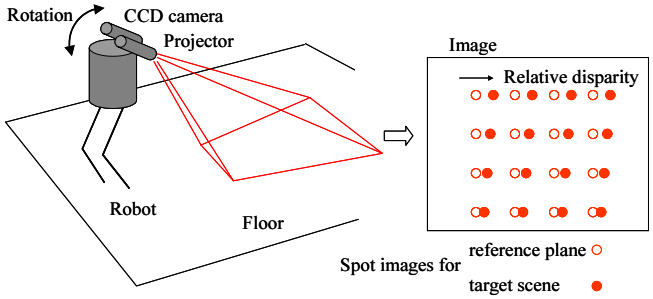

Fig. 1. Definition of a RDMap

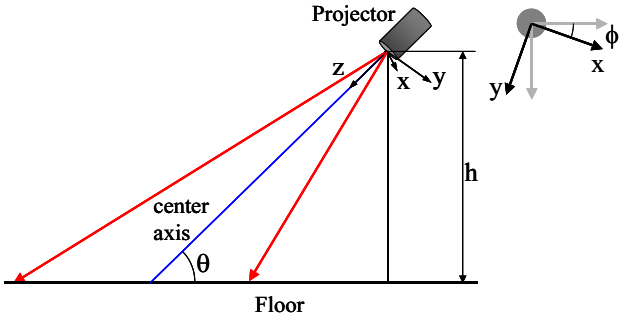

Fig. 2. Setting for detecting a RDMap

relative disparity $\Delta k = k - k_0$ is expressed as follows.

$$\Delta k\,(s,t) = \alpha\left(\frac{\cos\theta\sin\phi}{h} - \frac{\cos\theta_0\sin\phi_0}{h_0}\right)s + \alpha\left(\frac{\cos\theta\cos\phi}{h} - \frac{\cos\theta_0\cos\phi_0}{h_0}\right)t + \alpha\left(\frac{\sin\theta}{h} - \frac{\sin\theta_0}{h_0}\right) \quad (1)$$
$$\alpha = \frac{b\cdot f}{p}$$

b: baseline length (distance between the projection center and the lens center)

f: focal length of the lens of the CCD camera

p: width of each pixel of the CCD

This equation shows that the relative disparity is linear for s and t and, therefore, forms a plane in the $s-t$ space, which means that a plane in real 3D space also becomes a plane in the RDMap. With this fact, it can be determined whether or not a scene is planar by checking the RDMap.

The detection of a plane in the RDMap has the following advantages for using an ordinary range image. First, calibration of the sensor is greatly simplified. When the parameters of the plane are unnecessary, almost no calibration is needed. Secondly, the RDMap has homogeneous characteristics compared to an ordinary range image; the s,t values and the dispersion of errors of the values in the vertical axis (i.e., relative disparities) are constant regardless of the distance, which can make post-processing (e.g., Hough Transform) work better. Ordinary range images differ with regard to the density of points relative to distance and the error of the measured distance, which increases proportionally to the square of the distance. Although the method does not utilize the full information of range images, it is better for the restricted purpose of detecting planar regions.

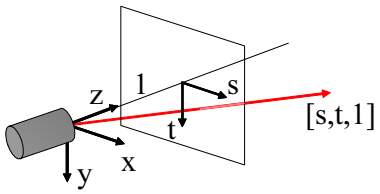

Fig. 3. Measuring direction

B. Measurement of the pose using a relative disparity map

When the parameters of the reference plane h_0, θ_0, ϕ_0 are given and the sensor is calibrated, i.e., α in (1) is obtained, h, θ, and ϕ of the target plane can be measured as follows. First, fit the plane to the RDMap by the least-squares method and obtain the parameters of the fitted plane,

$$\Delta k = As + Bt + C, \quad (2)$$

$$\begin{Bmatrix} A \\ B \\ C \end{Bmatrix} = \begin{bmatrix} \sum s^2 & \sum s\cdot t & \sum s \\ \sum s\cdot t & \sum t^2 & \sum t \\ \sum s & \sum t & n \end{bmatrix}^{-1} \begin{Bmatrix} \sum s\cdot\Delta k \\ \sum t\cdot\Delta k \\ \sum \Delta k \end{Bmatrix}.$$

From (1) and (2),

$$\frac{\cos\theta\sin\phi}{h} = \frac{A}{\alpha} + \frac{\cos\theta_0\sin\phi_0}{h_0} \equiv p \quad (3)$$

$$\frac{\cos\theta\cos\phi}{h} = \frac{B}{\alpha} + \frac{\cos\theta_0\cos\phi_0}{h_0} \equiv q \quad (4)$$

$$\frac{\sin\theta}{h} = \frac{C}{\alpha} + \frac{\sin\theta_0}{h_0} \equiv r \quad (5)$$

are obtained. Then from (3), (4) and (5),

$$h = \frac{1}{\sqrt{p^2+q^2+r^2}} \quad (6)$$

$$\theta = \tan^{-1}\left(\frac{r}{\sqrt{p^2+q^2}}\right) \quad (7)$$

$$\phi = \tan^{-1}\left(\frac{p}{q}\right) \quad (8)$$

are satisfied. Using (6), (7), and (8), the pose parameters h, θ and ϕ are calculated from the RDMap.

III. Small Range Image Sensor

Fig.4 shows the constructed prototype of the range image sensor attached on a humanoid Fujitsu HOAP-2. The laser projector is a Moritex SNF-519X (originally StockerYale's [13]). The wavelength of the laser is 670nm, and its power is 10mW. It projects 19×19, with a total of 361 spots. Because of the CCD camera's field of view, 15×15 spots are used. The angle between adjacent spots is 0.77deg. The CCD camera is a Toshiba IK-M41MR with a f=15mm lens. A Hoya R64 filter is attached to the lens of the CCD camera, and disturbance light with wavelength less than 640nm is cut. The baseline length is 23mm. The CCD camera is rotated with an angle of 18.5deg to avoid the correspondence problem [11]. A Hitachi IP-5005 is used

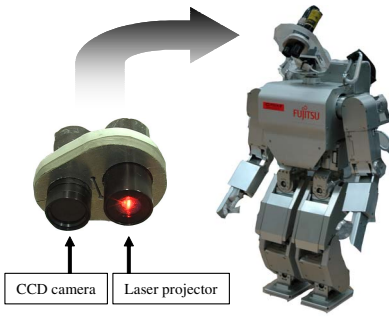

Fig. 4. A small range image sensor on a humanoid

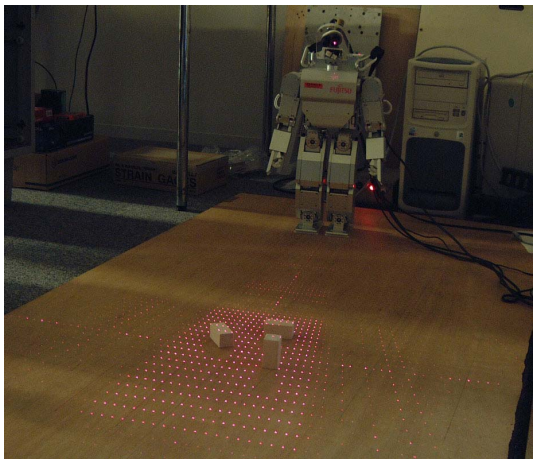

Fig. 5. Experimental scene

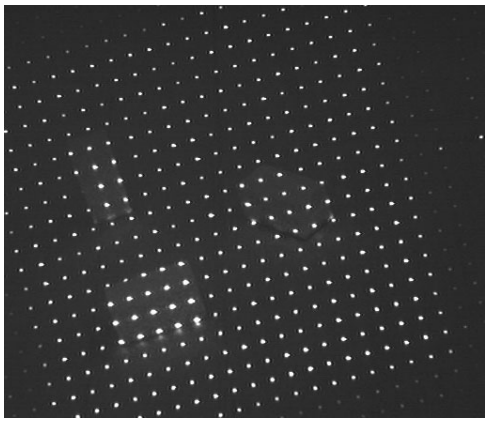

Fig. 6. An image for Fig.5 obtained by the CCD camera of the sensor

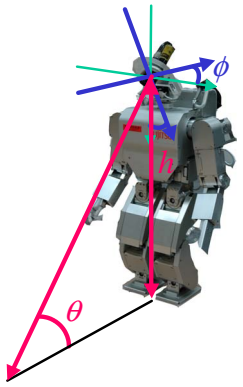

Fig. 7. Pose parameters of a range image sensor on a humanoid

for image processing, such as for the detection of spots and measurement of their center of gravity.

Fig.5 shows an example of an experimental scene. Obstacles are put on a flat floor, and the sensor projects spots on the floor. And Fig.6 is an image for Fig.5 obtained by the CCD camera. An RDMap is obtained from such an image.

IV. Fundamental Experiments Involving a Relative Disparity Map

A. Detection of obstacles by plane fitting

We first show experimental results to detect obstacles by plane fitting. Fig.7 shows the pose parameters of the sensor attached on the humanoid (same as Fig.2). The parameters are changed as shown in Table I by rotating the humanoid's head. ϕ was fixed to 0.

Fig.8 shows the RDMaps of a flat floor for the three conditions in Table I. It is shown that the RDMaps remain planar when the sensor pose is changed.

On the other hand, Fig.9 shows the RDMap with obstacles of 25(height)$\times$50$\times$25mm^3 for condition 2. Fig.9(b) corresponds to Figs.5, 6. One of the obstacles in Fig.9(b) was set so that its height would be 50mm. It is shown that the disparities at the obstacle are out of the plane. Fig.10 shows the residual sum of squares (RSS) for the plane fitted to the RDMaps We can see that the RSS is about 50pixel^2 or less for every condition without an obstacle (i.e., a flat floor) and larger than 100pixel^2 when obstacles are present. This shows that we can judge if there are obstacles or not from a RDMap only using RSS. This shows that the presence of obstacles can be determined with the exclusive use of RSS of an RDMap.

B. Measurement of a pose

We measured h, θ, and ϕ from the plane fitted to the RDMaps using (3), (4), and (5). The experiments were conducted ten times for each condition given in Table I. The results are shown in Fig.11.

It is verified that the pose can be measured from the RDMap only. The maximum errors for h, θ, and ϕ were

TABLE I
Experimental Conditions for the Detection of Obstacles by Plane Fitting

Condition	θ(deg)	h(mm)
Reference	45	480
1	30	490
2	35	485
3	40	481
4	45	480
5	50	474
6	55	470
7	60	464

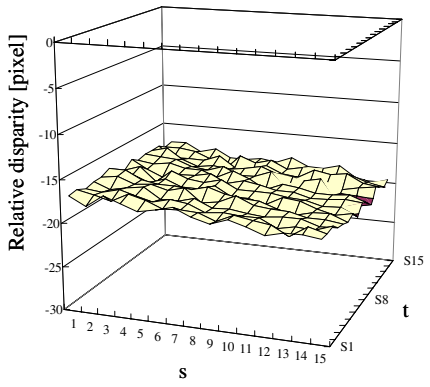

(a) condition1

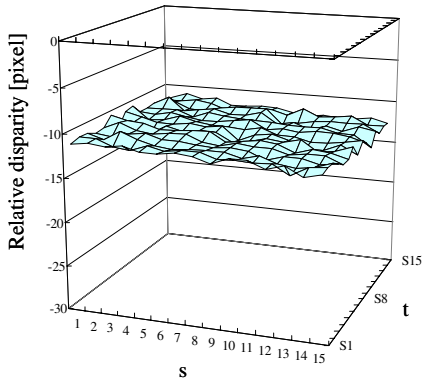

(b) condition2

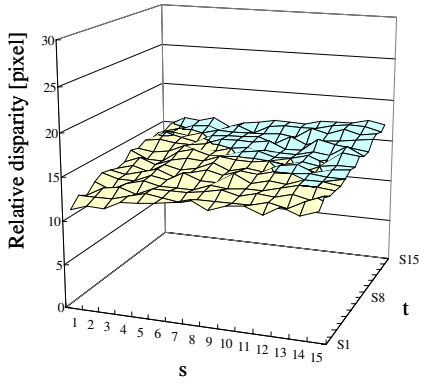

(c) condition7

Fig. 8. RDMap for several sensor poses

16.7mm, 2.67deg, and 1.67deg respectively. We consider these values to be small, i.e., the measurement works well. However, the errors may be reduced with error analysis. In addition, experiments with changing ϕ (which was set to zero because of the humanoid's mechanical constraint) should be performed. Errors of measurement of the plane when there are obstacles should be evaluated.

V. Experiments involving obstacle detection by a moving humanoid

The experiments in the previous section were performed statically, i.e., the humanoid was not moving. In this section,

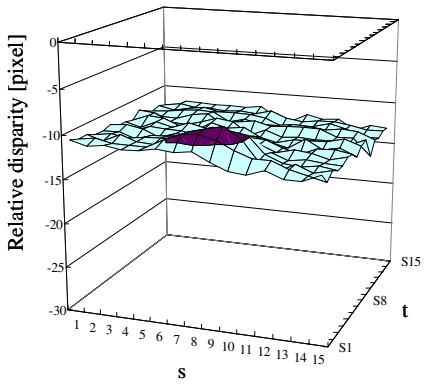

(a) One obstacle

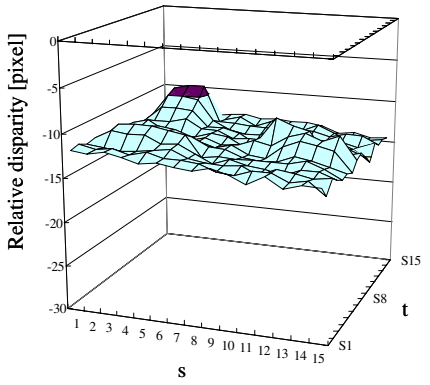

(b) Three obstacles

Fig. 9. RDMap with obstacles for condition 2

we show experimental results with the moving humanoid.

A. System configuration

Fig.12 shows a system to control a humanoid with the small range image sensor. The PC is a DELL Dimesion1100 (Pentium4 2.8GHz), and the OS is an RT-Linux (Kernel2.4.18-pre1). The small range image sensor is controlled by the same PC, and it works in the user space of the RT-Linux.

Fig.13(a) and (b) show the process flow while walking and when stopping respectively. The image process thread and socket thread are paralleled using a POSIX thread. They synchronize and communicate via Mutex. The socket thread and the software to control the humanoid (Fujitsu NueROMA OptionLibrary) are connected with a socket.

B. Experimental results

The humanoid started walking, found an obstacle and stopped. Fig.14(a) and (b) show the first (started) and last (stopped) scene. In the last scene, some of the spots are on the obstacle. Fig.15 shows the transition of the RSS of plane fitting when an obstacle was captured in the field of view. The RSS values before the obstacle was observed are less than 50pixel^2, and those after the obstacle was observed are much larger, i.e., more than 1000pixel^2. This shows that obstacles can be detected with the proposed method

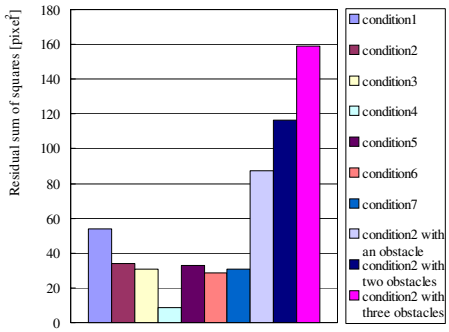

Fig. 10. RSS without/with an obstacle

even when a humanoid is walking. The RSS when there is an obstacle is larger than that in Fig.10 because the obstacle is larger. The system could detect an object as small as 5(height)×20×60mm^3. The processing time is now rather slow, i.e., 450ms. This is assumed to be because the NueROMA OptionLibrary with GUI has a large calculation cost. Improvement in this respect is necessary.

VI. Conclusion

In this paper, we proposed simple methods for recognizing obstacles on a plane using an RDMap that consists of disparities relative to a reference plane. We introduced a method to detect planar regions and obstacles by fitting a plane to the RDMap and a method to obtain the pose parameters from the RDMap only. Through fundamental experiments, we verified that a plane in real 3D space becomes a plane in the RDMap and that obstacles can be detected by using the RSS for the fitted plane, and we evaluated the measurement errors of measuring pose parameters. We constructed an experimental system with a humanoid and a small range image sensor and showed that the humanoid can detect obstacles on a plane by the proposed methods while walking.

Future work will include the introduction of a robust estimator such as LMedS for properly separating the plane and obstacles, the improvement of the control system of the humanoid to reduce the processing time, and more error analysis of the RDMap.

References

[1] K. Okada, S. Kagami, M. Inaba and H. Inoue, Plane Segment Finder: Algorithm, Implementation and Applications, Proc. 2001 IEEE International Conference on Robotics and Automation (ICRA'01), pp. 2120–2125, 2001.

[2] N. Pears and B. Liang, Ground Plane Segmentation for Mobile Robot Visual Navigation, Proc. 2000 IEEE/RSJ International Conference on Intelligent Robots and System(IROS 2001), pp.1513–1518, 2001!%

[3] For example, Point Grey Research Inc. http://www.ptgrey.com/

[4] T. Kanade, Development of a Video-Rate Stereo Machine, Proc. 1994 ARPA Image Understanding Workshop (IUW'94), pp.549–558, 1994.

[5] R. Ozawa, et al.!$Using Visual Odometry to Create 3D Maps for Online Footstep Planning!$Proc. of IEEE International Conference on Systems, Man and Cybernetics (SMC2005), pp. 2643–2648, 2005.

[6] J.A. Beraldin, F. Blais, M. Rioux, J. Domey and L. Cournoyer, A Video Rate Laser Range Camera for Electronic Boards Inspection, Proc. Vision '90 Conference, pp.4-1–4-11, 1990.

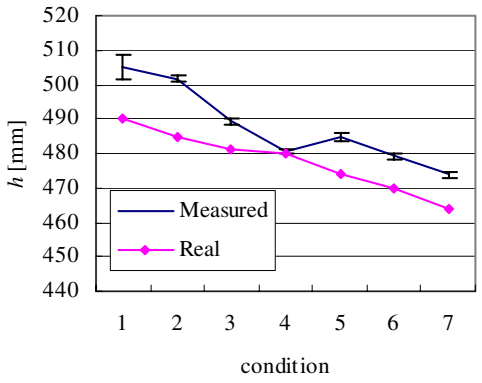

(a) h

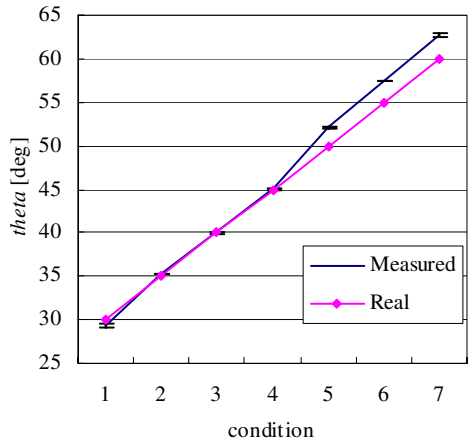

(b) θ

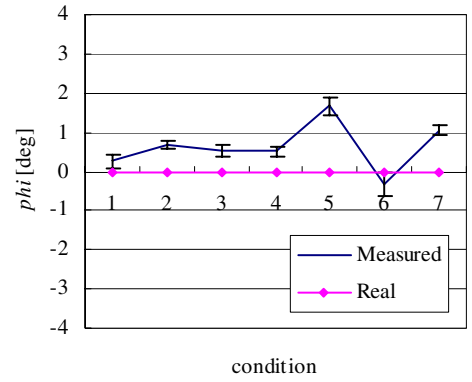

(c) ϕ

Fig. 11. Measurement of the pose parameters

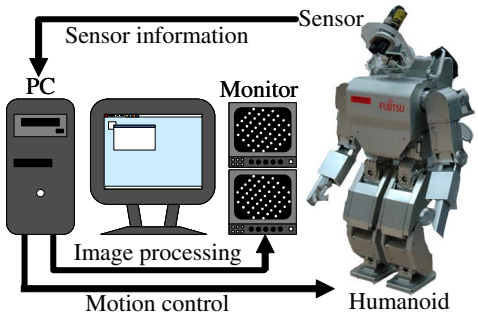

Fig. 12. Integrated system for controlling the humanoid

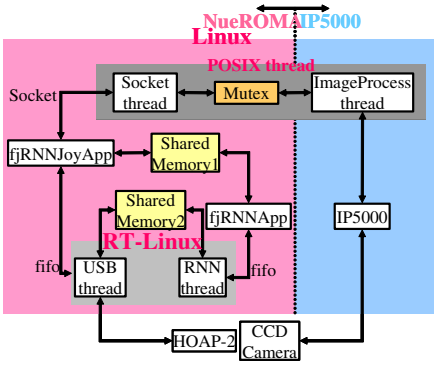

(a) While walking

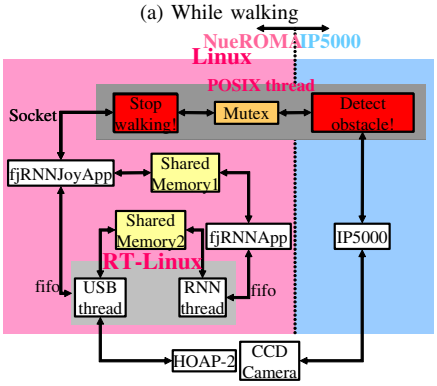

(b) When stopping

Fig. 13. Flowchart for controlling the humanoid

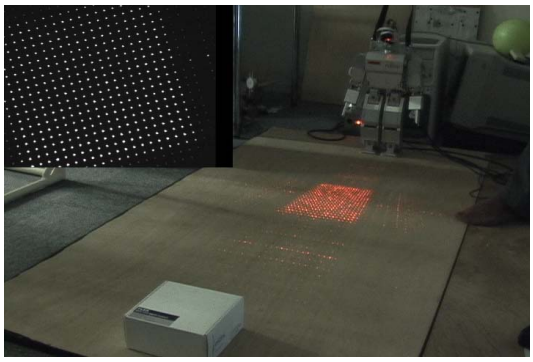

(a) Start

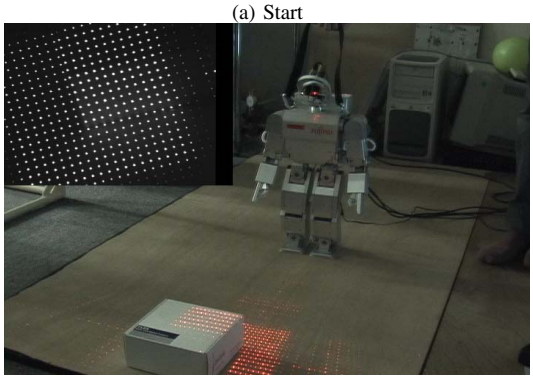

(b) Stop

Fig. 14. Experimental scene of a humanoid's obstacle detection

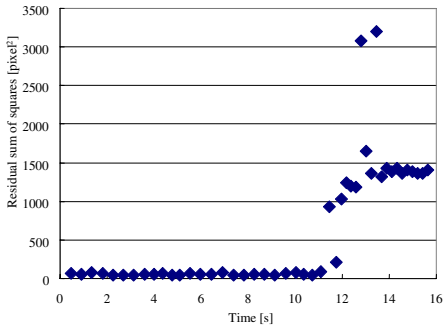

Fig. 15. Transition of the RSS while a humanoid is walking

[7] T. Kanade, A. Gruss and L.R. Carley, A VLSI Sensor Based Rangefinding System, Robotics Research Fifth International Symposium, pp.49-56, 1990.
[8] K. Nakazawa and C. Suzuki, Development of 3-D robot Vision Sensor with Fiber Grating: Fusion of 2-D Intensity Image and Discrete Range Image, Proc. 1991 International Conference on Industrial Electronics, Control and Instrumentation (IECON '91), pp.2368–2372, 1991.
[9] T. Tsubouchi, S. Takaki, Y. Kawaguchi and S. Yuta, A Straight Pipe Observation from the Inside by Laser Spot Array and a TV Camera, Proc. 2000 IEEE/RSJ International Conference on Intelligent Robots and Systems(IROS 2000), pp.82–87, 2000.
[10] Y. Miyazaki, A. Ohya and S. Yuta, Obstacle Avoidance Behavior of Autonomous Mobile Robot Using Fiber Grating Vision Sensor, Proc. 2000 IEEE International Conference on Industrial Electronics, Control and Instrumentation, pp.1925-1930, 2000.
[11] K. Umeda, A Compact Range Image Sensor Suitable for Robots, Proc. 2004 IEEE International Conference on Robotics and Automation (ICRA'04), pp. 3167–3172, 2004.
[12] M. Tateishi and K. Umeda, Construction of a Versatile Compact Range Image Sensor, Proc. 7th Int. Conf. on Quality Control by Artificial Vision (QCAV2005), pp.265–270, 2005.
[13] StockerYale, Inc. http://www.stockeryale.com/